Journal of Medical Engineering & Technology

ISSN: 0309-1902 (Print) 1464-522X (Online) Journal homepage: http://tandfonline.com/loi/ijmt20

A low cost stereophotogrammetric system for the evaluation of tridimensional head translations during visual tasks

Cláudia de Almeida Ferreira Diniz, Marcus Vinícius Faleiro de Andrade, Bruno Philip Alves da Silva, Maria Lúcia Machado Duarte, Lázaro Valentin Donadon, Ricardo Guimarães & Márcia Guimarães

To cite this article: Cláudia de Almeida Ferreira Diniz, Marcus Vinícius Faleiro de Andrade, Bruno Philip Alves da Silva, Maria Lúcia Machado Duarte, Lázaro Valentin Donadon, Ricardo Guimarães & Márcia Guimarães (2018): A low cost stereophotogrammetric system for the evaluation of tridimensional head translations during visual tasks, Journal of Medical Engineering & Technology, DOI: 10.1080/03091902.2018.1529203

To link to this article: https://doi.org/10.1080/03091902.2018.1529203

Published online: 22 Nov 2018.

JOURNAL OF MEDICAL ENGINEERING & TECHNOLOGY
https://doi.org/10.1080/03091902.2018.1529203

Taylor & Francis
Taylor & Francis Group

RESEARCH ARTICLE

A low cost stereophotogrammetric system for the evaluation of tridimensional head translations during visual tasks

Cláudia de Almeida Ferreira Diniz[a,b], Marcus Vinícius Faleiro de Andrade[a], Bruno Philip Alves da Silva[c], Maria Lúcia Machado Duarte[d], Lázaro Valentin Donadon[d], Ricardo Guimarães[b] and Márcia Guimarães[b]

[a]LABBIO, DEMEC/UFMG: Bioengineering Laboratory, Mechanical Engineering Department, Universidade Federal de Minas Gerais, Belo Horizonte, Brazil; [b]LAPAN, DEMEC/UFMG: Laboratory for the Research Applied to Neurovision, Mechanical Engineering Department, Universidade Federal de Minas Gerais, Belo Horizonte, Brazil; [c]DEMEC/UFMG: Mechanical Engineering Department, Universidade Federal de Minas Gerais, Belo Horizonte, Brazil; [d]GRAVIHB/UFMG: Group of Acoustics and Vibration on Human Beings, Mechanical Engineering Department, Universidade Federal de Minas Gerais, Belo Horizonte, Brazil

ABSTRACT

A simple, low cost and easy-to-operate 3D stereophotogrammetry system was developed to measure the kinematic pattern of head stabilisation during visual tasks. The system differs from commercially available ones since it: (a) takes into account the gaze motor coordination characteristics and measures the head translations quantified at the point that best represents the translations caused by the eyes' movement during visual tasks, that is, the midpoint between the eyes; (b) offers minimum restriction to the head movement and minimum interference with it; (c) innovates when using the position coordinates produced by a free-online tracker software. The system was effective in recording the head movements and its RMS total error was 0.705 mm with ±0.808 mm standard deviation. This represents an RMS total error of 3.5%, considered satisfactory because it provided results with a confidence level higher than 95%. The system was effective to record differences in head movements of 11 individuals in open and closed eyes conditions and revealed the direction-specific feature of the head displacements size. The results showed that the system is a cost-effective and accurate alternative for studies needing to accurately measure head movements during visual tasks.

ARTICLE HISTORY
Received 2 April 2018
Revised 23 September 2018
Accepted 24 September 2018
Published online 12 November 2018

KEYWORDS
Head movement; stereophotogrammetry; kinematic; head kinematic; software

1. Introduction

The human visual exploration used in most tasks is performed by the accurate coordination of a binocular oculomotor system, whose movements are followed by head [1–4] and body simultaneous movements [5–10]. The gaze fixation on an object located in front of the observer is a seemingly simple task. However, it has complex kinematics because gaze fixation involves the cervical spine and set of oculomotor muscles coordination, in order to direct the head and the gaze in space. This coordination implies controlling the resultant of all muscular forces to keep the displacement over time close to zero [11,12], simultaneously in all head degrees of freedom (DOF) [13].

For some people, the visual exploration required in the daily living activities is very difficult. During this exploration, they complain about image distortions that produce discomfort resulting in the condition named visual stress (VS) [14–17]. In the VS, there is a loss of visual efficiency characterised by blurred vision sensation, inaccurate visual perception or physical discomfort sensation when attempting to perform visual tasks [16]. Other symptoms such as fatigue, headache, glare, colour printing or image movement are described by the individuals a few minutes after they begin the tasks [14,15,17]. These symptoms are reported by 36% of students who have reading difficulty [14,15] and up to 47% of dyslexic children [18].

The VS symptoms may be related to some difficulty in controlling the resultant of the muscular forces that stabilises the head, leading to a head movement pattern where the displacement over time is not close to zero. This is possible because muscle activation problems can impair the visual exploration and interfere with the functional performance [10]. This hypothesis leads to the need for investigating the head kinematics to clarify if the stabilisation pattern offers some risk to the visual performance.

CONTACT Cláudia de Almeida Ferreira Diniz claudiafdiniz@yahoo.com.br LAPAN, DEMEC/UFMG: Laboratory for the Research Applied to Neurovision, Mechanical Engineering Department, Universidade Federal de Minas Gerais, Av. Antônio Carlos, 6627 Pampulha, Belo Horizonte, MG 31270-901, Brazil.

To implement this research type, when selecting the kinematic registration method, the gaze functioning motor coordination characteristics should be taken into account. For that, the head position is taken as the reference structure for the visual system functioning [19]. From it, the gaze stabilisation takes simultaneously into account the eyes, head and neck's DOF, in each displacement direction [20]. The gaze control stabilisation depends on the eye/head system geometric parameters, on the fixation point distance [20] and on the gaze direction [19,20].

The eye/head system geometrical parameters determine that any head rotation around the three biodynamic axes causes eyes translation in the space. This is due to the fact that the eyes are distant from the head centre of mass and yet further away from the head centre of rotation on the spine [21,22]. For this reason, to quantify the head kinematics it is important to quantify these head movements at the point that best represents the translations caused to the eyes, defined as the midpoint between them [20,23]. This feature becomes a requirement that could be met by motion analysis systems that record the head from the front. Although it seems to be a simple solution, putting a camera or other recording system components in front of the eyes could stimulate the occurrence of gaze deviations which, in turn, could introduce unwanted head movements and lead to inappropriate conclusions. Thus, for the purpose addressed in this study, the solution to be used should obtain the kinematic record without measurement system components being placed in front of the individual [24].

Beside this first requirement, another eye/head system's feature defines a second measurement system requirement [24]. The characteristic refers to the asymmetric head mass distribution and to its centre of mass, located at the skull base, being an eccentric point in relation to the skull shape [21], 0.07 m distant from the rotation centres in the column [25]. This puts the head permanently on anterior unbalance, rotated in positive direction of the basicentric *Y*-axis [13]. Thus, the head equilibrium on this axis, achieved when the Frankfurt plane [26] stays horizontal and the face stays vertical, becomes a state of constant dependence on the energy addition to the static system. The energy that balances the system is kinetic and is produced by the torque of the upper nape portion muscles, which insert into the skull occipital condyles and turn them back in the negative direction of the *Y*-axis. This defines a first class lever in which the length of the lever arms changes the resulting weight on each system side and the head rotations produce the eye's translations in space [27]. The described feature determines that the measurement system used to investigate the head kinematics needs a further requirement: a design that minimally interferes with movement. Thus, no component with expressive weight should be placed on the head.

For kinematics analysis, stereophotogrammetric (SPG) systems have been used to reconstruct static or dynamic objects in three dimensions from the analysis of images obtained by cameras [28]. For human kinematic analysis, the SPG is considered a powerful method [28] already employed for dynamic reconstructions of musculoskeletal mechanics in an accurate and precise way [29]. It has been used to analyse gait [30], sports movements [31], cervical spine movements [32], head stabilisation during gait [33] and head position during cell phone use [34]. For static reconstructions, it has been used to analyse dental occlusion [35], masticatory mandibular movements [36] and for three-dimensional reconstructions of both face [37] and skull [38]. These previous studies, although applying SPG to the head, had no intention to evaluate the head movement during visual tasks. Thereby, until now, no SPG systems were found to record the 3D head movements that meet the abovementioned requirements [24]. Moreover, the SPG use is still limited by the high cost of commercially available systems [28,39]. However, such cost has been minimised because low-priced digital cameras have incorporated high-definition recording systems [29] enabling an adequate image acquisition rate to register human movements. Additionally, commercial SPG systems require complex assembly and calibration procedures, demanding controlled environments such as laboratories [28,39]. This requirement limits its clinical use when examining functional disorders of the biological systems.

In studies about human head motor behaviour during visual tasks, it is of paramount importance being able to use an accurate and light recording system that does not change the behaviour of the motor system. In this context, this study presents an SPG system developed to quantify the 3D head translations kinematics calculated at the midpoint between the eyes. The system developed in this work was designed to meet the requirements of head kinematics studies during visual tasks. Furthermore, the system is a low price alternative to commercial systems, is of simple and flexible operation and can be used in a clinical environment [24].

2. Methods

2.1. Experimental configuration

The system presented here [24] uses SPG with two digital cameras to record the movements of four passive markers placed on the head. The images are processed with free-online tracker software that provides the 2D coordinates of each marker. These coordinates are used by "in-house" developed software to reconstruct the 3D coordinates of each marker and then the 3D coordinates of the midpoint between the eyes, named point *O*. To calculate this point, without using any component that records the images of the person from the front, point *O* was calculated from a geometric model in which the head is represented by a rigid tetrahedral figure with the four vertices (Figure 1) located as follows:

- At the occipital area, on the head midline (point *A*);
- At the direction of the external border of the eye orbit on the left side of the head (point *B*);
- At the top of the skull, over the interaural axis, on the head midline where the basicentric *Z*-axis is projected (point *C*);
- Same position as point *B*, however, at the head's opposite side (point *D*).

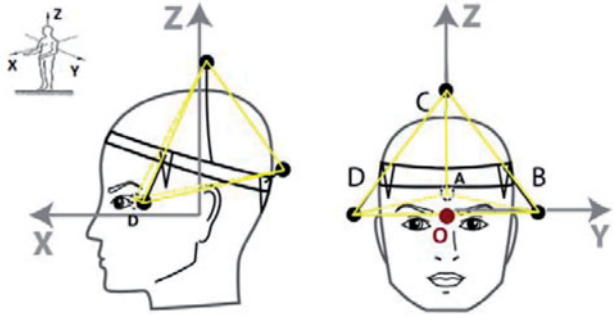

Figure 1. The rigid tetrahedral figure and the vertices' location. Point O is the midpoint between the eyes. Local and global systems are represented.

For this, the tetrahedral figure is reproduced on the head and one passive marker is placed at each vertex. The markers are mounted using four 20 mm diameter Styrofoam balls, four 50 mm metal rods, thermoplastic adhesive based on satin vinyl foam (EVA), coloured reflective paint, four hair clips, an elastic head strip, a metallic headband (Figure 2).

The assembly procedure is started by painting the Styrofoam spheres (markers) with reflective ink to facilitate their identification on the recorded videos. After drying, three balls (points *A*, *B* and *D*) are fixed in three metal rods with adhesive. The rods are then glued in three hair clips. A fourth ball (point *C*) already glued on metal rod was fixed with the same type of adhesive on a metallic headband. This headband was placed on the top of the head to position point *C* between points *B* and *D*. The assembly procedure ends with the hair clips with the markers being fixed to the elastic hair strip on the head so that each marker is in corresponding position to points *A*, *B*, *C* and *D* (Figure 3).

Since the head is considered a rigid body and the markers are pinned on it, the distances between them are assumed to remain constant (Figure 4).

In this model, point *O* is the midpoint between *B* and *D* vertices. The global system used for measuring the head movements corresponds to the *X*, *Y* and *Z* basicentric axis of a person's head in a standing position [40]. The local system of each marker is aligned to the global system. Each marker is identified by the letter corresponding to its vertex.

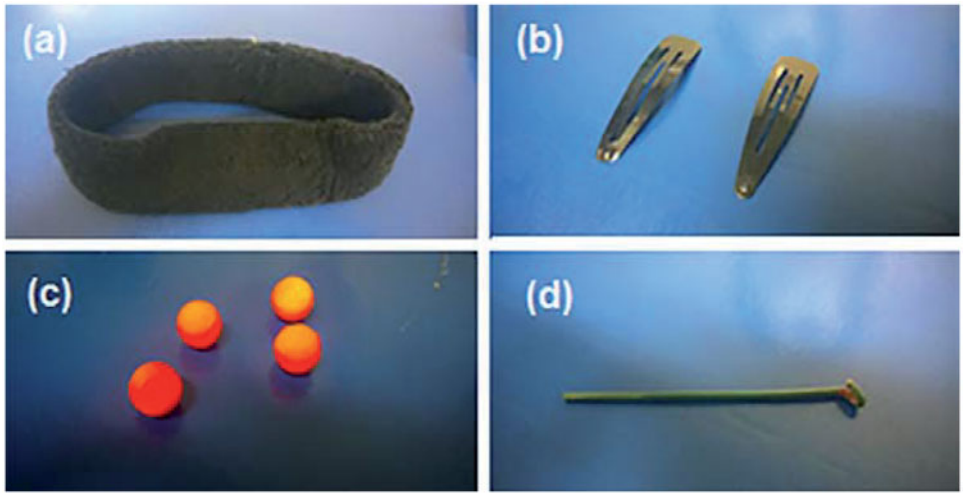

Figure 2. Material used for mounting the tetrahedral figure. (a) Elastic head strip. (b) Hair clips. (c) Styrofoam spheres painted. (d) Metal rod.

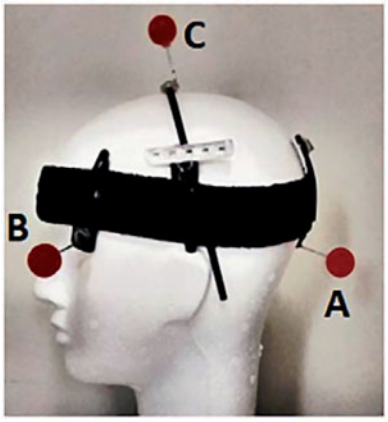

Figure 3. Side view of the markers attachment and known metric reference fixed on the elastic strip.

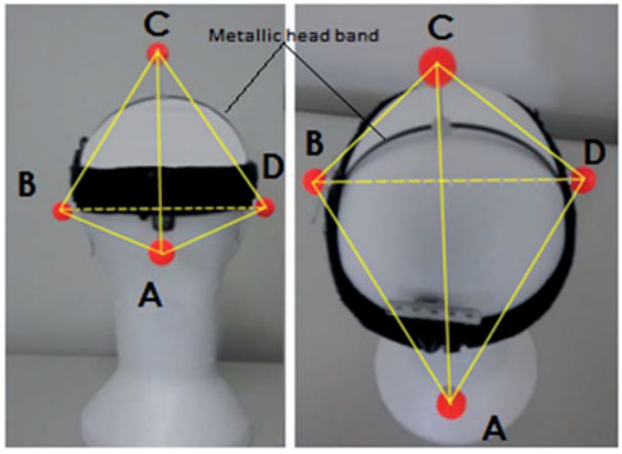

Figure 4. Tetrahedral figure mounted on head.

2.2. Image acquisition

The SPG system records the markers movements using two digital cameras model Canon EOS T5 (Canon Incorporation, Tokyo, Japan), fixed on tripods, orthogonally placed, positioned 2 m from the head, to record the head movements from the left (CAM1) and back (CAM2) sides (Figure 5). CAM1 height coincided with the ear's external acoustic meatus. This anatomical reference is considered the external projection of the head centre of mass [21]. CAM2 is placed at this same height.

The two videos are synchronised with the light emitting diode (LED) visible to both cameras that indicates the initial and final frames of the video. Together, the videos from both cameras record the positions of markers *A*, *B* and *C* in the *X*, *Y* and *Z* axes, but record the positions of marker *D* only in the *Y* and *Z* axes because it is not seen by CAM1. Therefore, *X* coordinate of point *D* is reconstructed.

The cameras are set to record with Full HD resolution with 1920 × 1080 screen lines, 30 frames per second and automatic selection of luminosity and focus. In this configuration, the optical system

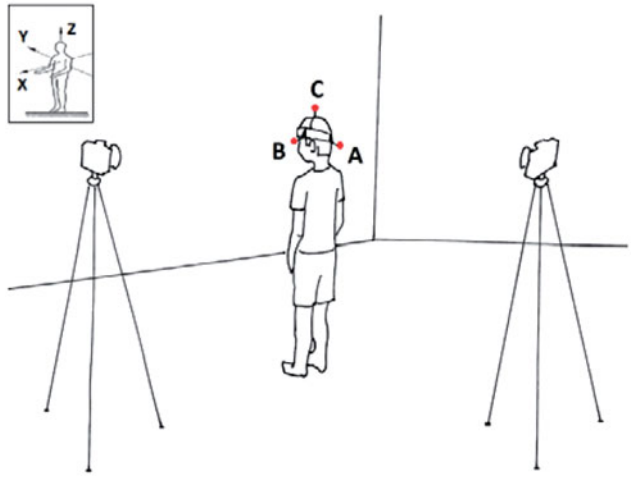

Figure 5. Representation of the cameras position in the SPG system.

distortion error calculated by triangles' similarity method was 1%. CAM1 registers markers *A*, *B* and *C*, and CAM2 registers markers *A*, *B*, *C* and *D* images.

2.3. Image processing

After recording, the markers' images are processed on a micro-computer with a tracker software (Tracker Video Analysis and Modeling Tool software, version 4.87, Open Source Physics) chosen for being an open source software, of simple use and with all the necessary features for the desired development. The Tracker software provides the bidirectional coordinates of each marker in each frame of the video.

Each marker was tracked in all 900 video frames recorded (30 fps during 30 s). The Cartesian system origin provided by the software for image analysis is configured so that, for CAM1 video, the origin is located at the ear's external acoustic meatus. For CAM2 video, the origin for the horizontal axis is aligned with the same height as for the horizontal axis of CAM1, and for the vertical axis it is at the head midline. These calibration procedures are performed at the initial frame of the original videos. Tracker slowest evolution rate is used to ensure a high matching level, avoiding drift. To prevent false identifications, the highest value allowed by the programme for automatic tracking is selected.

The tracking produces bi-dimensional coordinates of points *A*, *B*, *C* and *D*. CAM1 images directly produce *X* and *Z* coordinates for points *A*, *B* and *C*. Similarly, CAM2 images produce *Y* and *Z* coordinates of points *A*, *B*, *C* and *D*. As *Z*-coordinates are obtained by both cameras and the correlation between the data was very strong ($r = 0.999$) by Pearson's correlation coefficient (SPSS, version 21, SPSS Inc., Chicago, IL) [41], CAM2 data were chosen for the *Z*-axis coordinates.

2.4. Data analysis

After processing the images, the data of each marker are exported to an in-house developed software [24]. The algorithm assembles the 3D coordinate for each marker, reconstructs the *X*-axis coordinate for D marker, since it is not directly obtained, and also reconstructs the 3D coordinates of point *O*.

To reconstruct the *X*-axis coordinate for the D marker, it is assumed that all points belong to the R3 space and the distances between them remain constant. The distances to point *D* (D_{AD}, D_{BD}, and D_{CD}) are measured by the researcher with one metric reference and registered for further use.

For reconstruction the *X* coordinate of point *D*, a generic 3×3 M_{PQ} matrix is created, as shown in Equation (1).

$$M_{PQ} = \begin{bmatrix} D_{PQ}^2 & Y_Q - Y_P & Z_Q - Z_P \\ Y_Q - Y_P & 1 & 0 \\ Z_Q - Z_P & 0 & 1 \end{bmatrix} \quad (1)$$

The determinant of this matrix (Equation (2)) represents the square of the difference between the *X* coordinates of two generic points *P* and *Q* where $P = (X_p, Y_p, Z_p)$ and $Q = (X_q, Y_q, Z_q)$.

$$detM_{PQ} = D_{PQ}{}^2 - (Y_p - Y_q)^2 - (Z_P - Z_q)^2 = (X_p - X_q)^2 \quad (2)$$

Considering the generic points *P* and *Q*, as *A*, *B*, *C* and *D*, the above determinant is applied to *AB*, *BD* and *CD* pairs. These, together with the *X* coordinates of points *A*, *B* and *C*, are applied in Equation (3) so to give six approximate values for the *X* coordinates of point *D*.

$$\begin{bmatrix} X_{D1} \\ X_{D2} \\ X_{D3} \\ X_{D4} \\ X_{D5} \\ X_{D6} \end{bmatrix} = \begin{bmatrix} 1 & 1 & 0 & 0 & 0 & 0 \\ 1 & -1 & 0 & 0 & 0 & 0 \\ 0 & 0 & 1 & 1 & 0 & 0 \\ 0 & 0 & 1 & -1 & 0 & 0 \\ 0 & 0 & 0 & 0 & 1 & 1 \\ 0 & 0 & 0 & 0 & 1 & -1 \end{bmatrix} \begin{bmatrix} X_A \\ (detM_{AD})^{1/2} \\ X_B \\ (detM_{BD})^{1/2} \\ X_C \\ (detM_{CD})^{1/2} \end{bmatrix} \quad (3)$$

All these six values are used to calculate the modulus of vectors *AD*, *BD* and *CD*. These modules and the measured distances D_{AD}, D_{BD} and D_{CD} are used to calculate the approximate errors for every *X* value of point *D* (Equation (4)).

$$\begin{bmatrix} \Delta_{AD} \\ \Delta_{BD} \\ \Delta_{CD} \end{bmatrix} = \begin{bmatrix} D_{AD} - |AD| \\ D_{BD} - |BD| \\ D_{CD} - |CD| \end{bmatrix} \quad (4)$$

The three obtained error values are transformed in a total error Δ for every possible value of *X* (Equation (5)).

$$\Delta = \sqrt{(\Delta_{AD}^2 + \Delta_{BD}^2 + \Delta_{CD}^2)} \quad (5)$$

The chosen *X* coordinate value for point *D* is the one in which the calculated distance presents the smallest total error. Knowing the coordinates of points *A*, *B*, *C* and *D*, point *O* is reconstructed, as given by Equation (6).

$$O = \frac{B + D}{2} \quad (6)$$

The above formula is used at each time frame to calculate the *O* coordinates. The desired translations for point *O* are calculated as the total (Equation (7)) and instantaneous (Equation (8)) displacement vectors.

$$\Delta O = O(t) - O(0) \quad (7)$$

$$\Delta O_{inst} = O(t) - O(t-1) \quad (8)$$

At the end, all tridimensional point *O* positions are determined.

2.5. Experimental tests

Experimental tests were realised in two steps. First, they were tested for the identification of logic and signalling errors. The distortion caused by the proximity of the camera was disregarded. Markers *A*, *B*, *C* and *D* coordinates were manipulated for 450 instants, divided into three intervals of 100 instants with displacement, separated by three intervals of 50 instants without displacement. In the three displacement intervals, the data simulated an introduction of 20 mm cumulative translations in the *X*, *Y* and *Z* axes, with 0.2 mm displacement at each instant. The programme has been run. Measurements of the reconstruction of *D* point *X* coordinate showed a standard deviation of 0.013887 and a variance of 0.000193. The final calculation of the translations showed error of less than 0.0007 mm, which represents precision higher than that required for human body movements.

Next, the SPG system error was compared with the error of another system. As there was no other SPG systems for such a test, the movement values performed by a Styrofoam human head fixed on a robot model Motoman SK6 (produced by Scott Technology Ltd. Company, Dunedin, New Zealand [42]) were used to compare as “standard value” or “real value”. The ending point of the robot was placed over point *O* of the Styrofoam head. It was moved linearly by 20 mm, eight times, in each axis. The values for average repetitive error (ε), standard deviation (σ), minimum repetitive error (σ_{min}), maximum repetitive error (ε_{max}) and total RMS error of the reconstruction were calculated (Table 1). Calculation of the measurement

Table 1. Errors of the SPG system.

	Measured translations (mm)			
Robot movement axis	*X*-axis	*Y*-axis	*Z*-axis	RMS total error
X				
$\varepsilon_{,x}$	0.914	0.223	0.220	0.705
σ	0.039	0.083	0.147	
$\varepsilon_{,min}$	0.848	0.148	0.042	
$\varepsilon_{,max}$	0.974	0.398	0.558	
u_c	0.765	0.766	0.773	
Y				
$\varepsilon_{,y}$	0.968	0.574	0.481	
σ	0.202	0.265	0.201	
$\varepsilon_{,min}$	0.462	0.054	0.208	
$\varepsilon_{,max}$	1.172	0.937	0.926	
u_c	0.790	0.808	0.784	
Z				
$\varepsilon_{,z}$	0.717	0.721	0.568	
σ	0.043	0.175	0.201	
$\varepsilon_{,min}$	0.631	0.401	0.308	
$\varepsilon_{,max}$	0.757	0.907	0.979	
u_c	0.780	0.790	0.790	

ε: repetitive error; σ: repetitive error standard deviation; $\varepsilon_{,min}$: minimum repetitive error; $\varepsilon_{,max}$: maximum repetitive error; U_C: standard measured uncertainty.

uncertainty took into account the calibration of the robot and the resolution of the metric reference used to record the distances between the markers.

The system RMS total error corresponded to 3.5%, with an estimated standard deviation of ±0.808 mm.

2.6. Field testing

The SPG system was field-tested to measure the head movements of 11 individuals. The head movements were recorded during 30 seconds, once with open eyes, followed by with closed eyes. Gross error sources were minimised by using individuals positioning standardisation procedures. During the measurements, the individuals were instructed to stand in a quiet position, heads up and looking straight ahead. The feet were positioned in a standardised way according to the French Association of Posturography [43] which recommends 2 cm distance between the heels and 20° lateral deviation of the forefoot. Tests in which individuals have changed the position of the gaze, trunk, feet or flexed knees were discarded and repeated. For the closed-eye tests, one person was positioned to the right of the subject and the other to the left to hold him/her if he/she became unbalanced. Sources of error due to environmental factors were minimised with standardisation measures. The system was used always in the same 20 °C heated room, with low noise level, without natural light incidence and artificially lit by two 40 W fluorescent lamps fixed to the ceiling. The measured illuminance of the room was 14 lux.

The procedure used in this test was previously approved by the ethics committee of the Universidade Federal de Minas Gerais (UFMG)/Brazil, under protocol CAAE No. 50707815.6.0000.549 and the participants signed the free consent form before each test.

Table 2. Head translations' mean values at each movement axis, with open and closed eyes conditions.

	X-axis		*Y*-axis		*Z*-axis	
Visual condition	Mean	SD	Mean	SD	Mean	SD
EC	16.5	21	3.35	2.37	1.12	1.11
EO	6.04	5.65	4.16	3.18	0.93	0.52

Trans.: translations; SD: standard deviation; EC: eyes closed; EO: eyes opened.

For the tests, the system was assembled and the cameras were set to record at Full HD resolution, 60 frames per second and with automatic selection of brightness and focus control. They were fixed on tripods at 2 m distance from the head and orthogonally positioned to film it from the left (CAM 1) and from behind (CAM 2), respectively, as presented in Figure 5. In this configuration, the image distortion error by the optical system estimated with the triangles similarity method for 20 mm translations was 1%.

For image processing, the following specifications were applied to the tracking programme: minimum similarity score required for automatic tracking without false identifications selected with the highest value allowed by the programme; tracker evolution rate set to the minimum value allowed by the programme to ensure a high level of match and to avoid drift.

3. Results

Seven women and four men, aged 13–21 years (16.4 ± 2.4 years) participated in the tests. Despite the individuals trying to stay with the head in quiet position, point *O* data calculated by the SPG system showed that the middle point between the eyes of individuals moved in translations, simultaneously, in all axes, due to the head movement. The mean values for each axis of movement, with the EO (eyes opened) and EC (eyes closed) test conditions are shown in Table 2.

Figure 6 shows the translational amplitude chart representation of each 1800 positions recorded during 30 seconds of EC and EO conditions, for all 11 individuals, so to illustrate the pattern of the sample.

4. Discussion

This study developed an SPG system that used simple, low-cost and easy-to-operate components and that took into account the gaze motor coordination

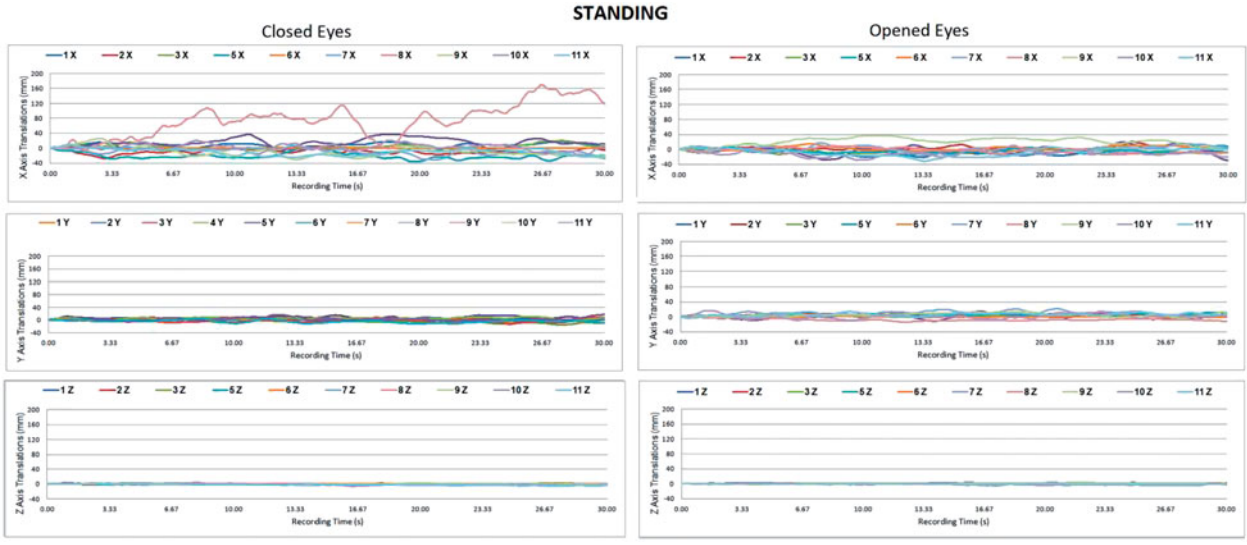

Figure 6. Results of point *O* positions by axis, during 30 seconds, for the 11 individuals in opened and closed eyes' test condition. The position in the start frame was named "zero". One to 11 is the individual's numbers.

characteristics. It was effective in evaluating the tridimensional head movements with an RMS total error of 3.5%. This error was satisfactory because it provided results with a confidence level higher than 95%.

The system has characteristics that made it unique compared with other systems developed to quantify head movements. One of its main characteristics is to measure the 3D movement at the middle point between the eyes with no system components in the frontal field of the individual. This avoids induced gaze deviations which could introduce unwanted head movements. No similar systems were found in the literature or in the market. For that reason, to compare this SPG system with other two camera commercial systems does not seem appropriate since, at the latter, in order to obtain point *O* coordinates, the cameras have to be placed in front of the eyes. This is not recommended for examining the human head motor behaviour during gaze coordination, because the sight direction is achieved with eye movements combined with head movements [2,4,44,45] that are produced in the rotational centres, far from the eyes [23].

To do this, software that reconstructs the coordinates of point *O* from head marker position data was developed [24]. The software uses the position coordinates produced by a free-online tracker software. This is an innovation of this system that reduced the total cost of the system, making it cost-effective. The SPG system developed by Castro et al. [46] although having a lower cost compared with other commercial systems requires the acquisition of up to eight cameras plus the software. Therefore, its total cost is superior to the system presented in this paper.

The use of a free-online tracker software is an innovation that requires caution by the operator because is a step that can introduce errors in the data if care is not taken. The software stops if any loss of tracking quality is detected. The software only continues when the operator manually corrects the tracking process. Such observation may make the process time-consuming and requires a trained operator. It is a system limitation. However, for studies with a reduced number of videos, the possibility of making low cost kinematic analysis has a benefit that exceeds this limitation.

The geometric model used at the algorithm to reconstruct the coordinates and calculate point *O* position vector and the orientation matrix in the tridimensional space was based in the concept of forward kinematic modelling of robots, which uses three DOF to position an ending point in space [47]. In the case of the human head, point *O* is the end point of the head mechanical system during visual tasks and its displacement in $\mathbb{R}^3$ is the result of the DOFs functional restriction for this mechanical system.

To offer minimum restriction to the head movement and minimum interference with the head movements, the markers' material selection and attachment method were determined by the head anatomy. The interference in the alignment caused by the head mass asymmetric distribution [21], and the uninterrupted force required to align it [13], determined that they should use markers whose total mass was less than 1% of the average head weight. The apparatus described by Panerai et al. [48], for example, used 0.370 kg sensors, mechanical components and helmet. When placed,

they add mass to the anterior portion of the head, modifying the kinematics being investigated.

This system has a limitation in addition to the aforementioned. The analysis of the uncertainty sources pointed out that the measure of the distances between the markers may contribute to the most expressive part of the uncertainty. When the operator carefully measures these distances, this limitation is minimised.

The system was effective in recording the head movements of the 11 individuals examined and it was sensitive to changes in the visual condition during the tests. This sensitivity was evidenced by the differences in translational averages in each axis obtained from open and closed eyes. This result confirms the specificity of the system here presented to record the kinematic head behaviour during visual tasks.

In addition, the SPG system presented here revealed a feature on kinematics of the head that has not yet been measured in other studies: the head displacements size is direction-specific. In this study, the largest translations were recorded on the *X*-axis, which coincides with the anteroposterior direction of body oscillation. This is the direction of greater oscillation amplitude when the individual is standing in the position used in that study. The smallest translations were recorded on the *Z*-axis, which is the vertical axis.

5. Conclusions

This paper has presented a low-cost SPG system developed for investigations of the human head movements that quantified in three dimensions the translation of the midpoint between the eyes. For its satisfactory accuracy, the developed system proved to be both suitable for use in clinical settings and sensible to changes in visual condition test. Therefore, it is an alternative system for conducting studies aiming quality and reduced cost.

Acknowledgements

The authors thank Prof. Dr. Pinotti M.B., in memoriam, first leader of this study.

Ethical approval

This study registered in the Universidade Federal de Minas Gerais Research Ethical Committee (number CAAE – 50707815.6.0000.549).

Disclosure statement

No potential conflict of interest was reported by the authors.

Funding

The only financial support during the course of the research was a scholarship from FAPEMIG (Fundação de Amparo à Pesquisa de Minas Gerais) received by the first author.

References

[1] Hess BJM, Thomassen JS. Kinematics of visually-guided eye movements. PLoS One. 2014;9:e95234.
[2] Freedman EG. Coordination of the eyes and head during visual orienting. Exp Brain Res. 2008;190:369–387.
[3] Kunin M, Osaki Y, Cohen B. Rotation axes of the head during positioning, head shaking, and locomotion. J Neurophysiol. 2007;98:3095–3108.
[4] Stahl JS. Eye-head coordination and the variation of eye-movement accuracy with orbital eccentricity. Exp Brain Res. 2001;136:200–210.
[5] Fogt N, Persson TW. A pilot study of horizontal head and eye rotations in baseball batting. Optom Vis Sci. 2017;94:789–796.
[6] Kanari K, Sakamoto K, Kaneko H. Effect of visual attention on the properties of optokinetic nystagmus. PLoS One. 2017;7:1–16.
[7] Richardson M, Schwarz B. Modal parameter estimation from operating data. Sound Vib. 2003;37:1–8.
[8] Niehorster DC, Cornelissen THW, Holmqvist K, et al. What to expect from your remote eye-tracker when participants are unrestrained. Behav Res Methods. 2018;50:215–227.
[9] You M, Yamane T, Tomita H, et al. A novel rat head gaze determination system based on optomotor responses. PLoS One. 2017;12:1–20.
[10] Srulijes K, Mack DJ, Klenk J, et al. Association between vestibulo-ocular reflex suppression, balance, gait, and fall risk in ageing and neurodegenerative disease: protocol of a one-year prospective follow-up study. BMC Neurol. 2015;15:192.
[11] Bertoz A. The brain sense of movement. Cambridge (UK): Harvard University Press; 2000. p. 337.
[12] Hogan N, Mussa-Ivaldi FA. Muscle behavior may solve motor coordination problems. In: Berthoz A, Vidal PP, Graf W, editors. The head-neck sensory motor system. Oxford: Oxford University Press; 1992. p. 151–157.
[13] Kapandji AI. Fisiología articular [Joint physiology]. 5th ed. Madrid: Editorial Médica Panamericana SA; 1999. p. 170–253.
[14] Loew SJ, Rodríguez CMNV, et al. Levels of visual stress in proficient readers: effects of spectral filtering of fluorescent lighting on reading discomfort. Span J Psychol. 2015;18:1–11.
[15] Loew SJ, Marsh NV, Watson K. Symptoms of Meares-Irlen/visual stress syndrome in subjects diagnosed with chronic fatigue syndrome. Int J Clin Heal Psychol. 2014;14:87–92.

[16] Wilkins A, Huang J, Cao Y. Visual stress theory and its application to reading and reading tests. J Res Read. 2004;27:152–162.
[17] Wilkins AJ, Lewis E, Smith F, et al. Coloured overlays and their benefit for reading. J Res Read. 2001;24: 41–64.
[18] Saksida A, Iannuzzi S, Bogliotti C, et al. Phonological skills, visual attention span, and visual stress in developmental dyslexia. Dev Psychol. 2016;52:1503–1516.
[19] Pozzo T, Berthoz A, Lefort L. Head stabilization during various locomotor tasks in humans. I. Normal subjects. Exp Brain Res. 1990;82:97–106.
[20] Panerai F, Sandini G. Oculo-motor stabilization reflexes: integration of inertial and visual information 1. Neural Netw. 1998;11:1191–1204.
[21] Sacco ICN, Tanaka C. Cinesiologia e Biomecânica dos Complexos Articulares. Rio de Janeiro: Editora Guanabara Koogan SA; 2008. p. 301–347.
[22] Ozaiz N, Nordim M, Fundamentals of biomechanics: equilibrium, motion and deformation. New York: Van Nostrand Reinhold; 1991. p. 1–396.
[23] Panerai F, Metta G, Sandini G. Visuo-inertial stabilization in space-variant binocular systems. Robot Auton Syst. 2000;30:195–214.
[24] Diniz CAF. Estudo estereofotogramétrico da cinemática da cabeça de indivíduos com Estresse Visual [dissertation]. Belo Horizonte (MG): Universidade Federal de Minas Gerais; 2017.
[25] Viviani P, Berthoz A. Dynamics of the head-neck system in response to small perturbations: analysis and modeling in the frequency domain. Biol Cybern. 1975; 19:19–37.
[26] Haiter-Neto F, Oliveira SS, Casanova MS, et al. Telerradiografias obtidas em posição natural da cabeça alteram as grandezas cefalométricas? Rev Dent Press Ortodon Ortop Facial. 2007;12:117–123.
[27] Nordim M, Frankel VH. Basic biomechanics of the musculoskeletal system. 2nd ed. Londres: Lea & Febiger; 1989. p. 209–223.
[28] Theriault DH, Fuller NW, Jackson BE, et al. A protocol and calibration method for accurate multi-camera field videography. J Exp Biol. 2014;217:1843–1848.
[29] Tzou CHJ, Artner NM, Pona I, et al. Comparison of three-dimensional surface-imaging systems. J Plast Reconstr Aesthetic Surg. 2014;67:489–497.
[30] Timmis MA, Turner K, Latham K. The effect of trial frames on adaptive gait. Gait Posture. 2015;41: 332–334.
[31] Mkaouer B, Jemni M, Amara S, et al. Effect of three technical arms swings on the elevation of the center of mass during a standing back somersault. J Hum Kinet. 2014;40:37–48.
[32] Wilke J, Niederer D, Fleckenstein J, et al. Range of motion and cervical myofascial pain. J Bodyw Mov Ther. 2015;49:1–4.
[33] Sessoms PH, Gottshall KR, Sturdy J, et al. Head stabilization measurements as a potential evaluation tool for comparison of persons with TBI and vestibular dysfunction with healthy controls. Mil Med. 2015;180: 135–142.
[34] Schabrun SM, Hoorn W, Van Den Moorcroft A, et al. Texting and walking: strategies for postural control and implications for safety. PLoS One. 2014;9:e84312.
[35] Maurer C, Stief F, Jonas A, et al. Influence of the lower jaw position on the running pattern. PLoS One. 2015; 10:e0135712.
[36] Karlsson S, Persson M, Carlsson GE. Mandibular movement and velocity in relation to state of dentition and age. J Oral Rehabil. 1991;18:1–8.
[37] Artopoulos A, Buytaert JAN, Dirckx JJJ, et al. Comparison of the accuracy of digital stereophotogrammetry and projection moiré profilometry for three-dimensional imaging of the face. Int J Oral Maxillofac Surg. 2014;43:654–662.
[38] Meyer-Marcotty P, Böhm H, Linz C, et al. Three-dimensional analysis of cranial growth from 6 to 12 months of age. Eur J Orthod. 2014;36:489–496.
[39] Detchev I, Mazaheri M, Rondeel S, et al. Calibration of multi-camera photogrammetric systems. Int Arch Photogramm Remote Sens Spatial Inf Sci. 2014;XL-1: 101–108.
[40] ISO 2631:1. Mechanical vibration and shock – evaluation of human exposure to whole body vibration; 1997. p. 1–39.
[41] SPSS Statistics version 21; New York (NY): IBM Corporation. 2014.
[42] SK6 Robot, Marion, Ohio: Scott Technology Ltd. Company; 2010.
[43] Ouaknine M. Cyber Sabot: the Statodynamic conception. Résonan Eur Rachis. 2009;16:2117–2128.
[44] Thumser ZC, Stahl JS. Eye-head coupling tendencies in stationary and moving subjects. Exp Brain Res. 2009;195:393–401.
[45] Land MF. The coordination of rotations of the eyes, head and trunk in saccadic turns produced in natural situations. Exp Brain Res. 2004;159:151–160.
[46] Castro JLG, Medina-Carnicer R, Martinez A. Design and evaluation of a new three-dimensional motion capture system based on video. Gait. 2006;24: 126–129.
[47] Rosário JM. Introdução à Robótica. In: Robótica industrial I – modelagem, utilização e programação. São Paulo (SP): Editora Baraúna; 2010. p. 21–48.
[48] Panerai F, Hanneton S, Droulez J, et al. A 6-dof device to measure head movements in active vision experiments: geometric modeling and metric accuracy. J Neurosci Methods. 1999;90:97–106.